ELSEVIER

Polymer 42 (2001) 737–746

polymer

www.elsevier.nl/locate/polymer

Effects of interfacial adhesion on the rubber toughening of poly(vinyl chloride) Part 1. Impact tests

Zhehui Liu[a,*], Xiaoguang Zhu[a], Lixin Wu[b], Ying Li[c], Zongneng Qi[b], Chungloong Choy[a], Fosong Wang[b]

[a]*Department of Applied Physics, Hong Kong Polytechnic University, Hung Hom, Kowloon, Hong Kong, People's Republic of China*
[b]*State Key Laboratory of Engineering Plastics, Institute of Chemistry, Chinese Academy of Sciences, Beijing 100080, People's Republic of China*
[c]*School of Resources and Engineering, Beijing University of Science and Technology, Beijing 100083, People's Republic of China*

Received 19 January 2000; received in revised form 9 March 2000; accepted 18 April 2000

Abstract

The influence of interfacial adhesion on the impact toughness of poly(vinyl chloride) (PVC)–nitrile rubber (NBR) blends with the morphology of well-dispersed rubber particles has been investigated. The blend containing NBR 18 (NBR with 18 wt% acrylonitrile (AN)) has medium interfacial adhesion strength, and exhibits a brittle–ductile transition at a critical matrix ligament thickness $T_c = 0.059$ μm while the blend containing NBR 26 (NBR with 26 wt% AN) and having stronger interfacial adhesion exhibits the transition at $T_c = 0.041$ μm. The difference can be understood in terms of the deformation mechanisms. Debonding at the interface of the PVC–NBR 18 blend takes place upon impact, and this induces shear yielding of the matrix. For the PVC–NBR 26 blend, however, no microvoid is formed, so the occurrence of matrix shear yielding is delayed. In the investigated rubber particle size range (0.04 − 0.12 μm), debonding followed by matrix shear yielding is a much more important toughening mechanism than internal cavitation of rubber particles. © 2000 Elsevier Science Ltd. All rights reserved.

Keywords: Interfacial adhesion; Brittle–ductile transition; Rubber toughened poly(vinyl chloride)

1. Introduction

Impact strength is one of the most important mechanical properties of plastic–rubber blends since it determines the utility of these materials. It is generally believed that the interfacial adhesion between the dispersed rubber particles and the matrix plays an important role in the toughening of polymers. The effect of interfacial adhesion on the impact strength has long been of great interest.

For a constant interfacial adhesion it has been widely reported that the impact strength is influenced by morphological parameters [1–30]. It has been found that the effects of the size, size distribution and volume fraction of rubber particles on the impact strength of a blend with the morphology of well-dispersed particles can be combined into the effect of a single parameter, the matrix ligament thickness (surface to surface interparticle distance) T [1–16]. It was proposed that the critical matrix ligament thickness T_c for the onset of brittle–ductile transition is a characteristic of the matrix for a given temperature and mode and rate of deformation [1,2]. A quantitative relationship between T_c and the intrinsic ductility of the polymer matrix was established based on the above assumption [4]. The particle spatial distribution parameter has a much more substantial influence on the impact strength of polymer blends. It is generally accepted that a blend with the morphology of agglomerated particles is brittle. It has been demonstrated that the pseudo-network morphology has a higher toughening efficiency than the morphology of well-dispersed particles [18–21]. As a result, the T_c value for poly(vinyl chloride) (PVC)–nitrile rubber (NBR) blends with the morphology of well-dispersed particles is smaller than that for the blends with the pseudo-network morphology [21]. Whether or not T_c depends on interfacial adhesion is also interesting.

It is believed that the effects of interfacial adhesion and morphological parameters on the impact strength are interrelated [23–25,28–48]. It has long been known that an increase in interfacial adhesion can lead to a reduction of

* Corresponding author. Tel.: +852-2766-5662; fax: +852-2333-7629.
E-mail address: aplzh@polyu.edu.hk (Z.H. Liu).

0032-3861/01/$ - see front matter © 2000 Elsevier Science Ltd. All rights reserved.
PII: S0032-3861(00)00375-X

average particle size and simultaneously an increase in impact strength. However, impact strength is not always increased by reducing particle size. If the particle size is so small that internal cavitation of rubber particles cannot take place, then the blend has a very low impact strength [29–36,49–52]. An increase in interfacial adhesion can also give rise to a more uniform dispersion of particles in a matrix [37–43], i.e. a change from the morphology of agglomerated particles to the pseudo-network morphology or the morphology of well-dispersed particles, which have different toughening efficiencies. The above effects of morphological parameters resulting from a change of interfacial adhesion are classified as an indirect effect of interfacial adhesion on toughening. On the other hand, a direct effect of interfacial adhesion would be the one when all other parameters (including morphological parameters) except interfacial adhesion are kept identical. Therefore, an understanding of the direct effect of interfacial adhesion alone requires the separation of effects of morphological parameters.

So far, there have been some suggestions on the direct effect of interfacial adhesion on rubber toughening. When both the rubber particle size and the rubber content are identical, enhancement of the interfacial adhesion can increase the impact strength of some polymer blends, i.e. polystyrene (PS)- functionlized NBR [23] and poly(methyl methacrylate)–rubber blends [24]. However, it has been suggested that interfacial adhesion does not have an influence on the impact strength of some other polymer blends, i.e. polyamide 6 (PA6)-ethylene propylene diene monomer (EPDM)-grafted-maleic anhydride (MA) [25] and PVC–methyl methacrylate–butadiene–styrene graft copolymer (MBS) [28].

The miscibility between PVC and NBR increases with the acrylonitrile (AN) content in NBR up to 40% by weight [32]. In other words, the interfacial adhesion between PVC and NBR can be enhanced through an increase in AN content. It has been established that there is an optimum AN content in NBR for achieving the highest impact strength in PVC–NBR blends [32,33]. The morphology of the PVC–NBR blends with the optimum AN content is mainly a continuous rubber network together with some dispersed rubber particles [32,33]. This complex morphology makes it difficult to find the toughness–interfacial adhesion relationship. On the other hand, we have successfully prepared PVC–NBR blends with the morphology of well-dispersed NBR rubber particles and the pseudo-network morphology, respectively [14,20,21]. The morphological parameters of a blend with the morphology of well-dispersed particles can be related by a simple equation [21,53–55], so we focus our attention on the morphology of well-dispersed particles in this investigation.

In this series of two papers, we study the direct effect of interfacial adhesion on the toughness of PVC–NBR blends measured at impact speed and at low speed of extension, respectively. In the present work, we investigate the effect of interfacial adhesion on the brittle–ductile transition of PVC–NBR blends with the morphology of well-dispersed rubber particles by keeping the morphological parameters identical. In particular, the effect of interfacial adhesion on the critical matrix ligament thickness T_c has been studied. We also investigate the deformation mechanisms of the above blends to elucidate how interfacial adhesion affects the impact strength of the blends.

2. Experimental

2.1. Materials

The polymers used in this study were a commercial grade PVC (grade S-1000, supplied by Qilu Petrochemical Company, People's Republic of China) with a number-average molecular weight Mn = 62 500, and two commercial NBRs (supplied by Lanzhou Chemical Company, People's Republic of China) containing 18 and 26 wt% of AN, respectively.

2.2. Blend preparation

The NBRs were labeled NBR 18 (containing 18 wt% AN) and NBR 26 (containing 26 wt% AN), respectively. PVC–NBR 18 blends were prepared as described in a previous paper [14]. PVC–NBR 26 blends were prepared under the same processing conditions as those for preparing PVC–NBR 18 blends. NBR 26a is the original commercial product. It was milled on a two-roller mill at a room temperature for 30 min to produce NBR 26b. NBR 26 was blended with PVC (containing 0.4 parts per hundred parts of resin (abbreviated as 0.4 phr) lubricator, 3 phr stabilizer, and 5 phr plasticizer) on the two-roller mill at 160°C for 6 min to give NBR 26 blends. The milled sheets were stacked together and compression-molded at 160°C for 10 min, then cooled slowly down to room temperature to give 4 mm thick plates. The samples for impact tests and morphological observations were cut from these plates.

2.3. Impact tests

Izod impact tests were performed at 16°C according to ASTM-D256.

2.4. Morphological observations

The Izod bars were immersed in liquid nitrogen and then fractured. The fracture surfaces were etched in an oxidizer composed of 100 ml H_2SO_4, 30 ml H_3PO_4, 30 ml H_2O, and 3 g $K_2Cr_2O_7$ at 30°C for 5 min to remove the rubber phase. They were then coated with gold. The morphologies were observed on a Hitachi S-530 scanning electron microscope (SEM).

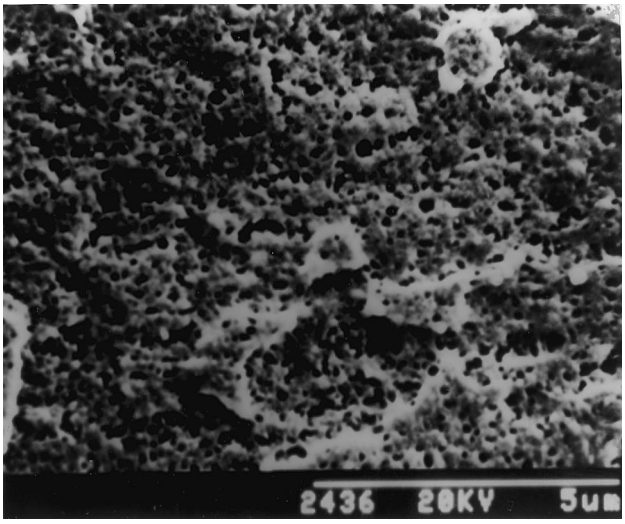

Fig. 1. SEM micrograph of a PVC–NBR26 blend, showing the morphology of well-dispersed rubber particles.

2.5. Analysis of morphological parameters

The particle size and particle size distribution were obtained from SEM micrographs using a computerized image analyzer. For each sample, 300–400 rubber particles were analyzed and the number-average particle size was obtained.

2.6. Measurement of glass transition temperatures of rubbers

A Perkin–Elmer TMS-2 thermo-mechanical analyzer was used to measure the glass transition temperatures of NBR rubbers by heating the sample from −100 to 20°C at a rate of 20°C min^{-1}.

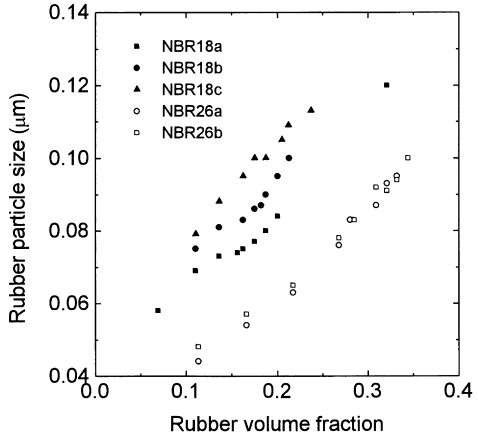

Fig. 2. Rubber particle size versus rubber volume fraction for PVC–NBR blends with the morphology of well-dispersed rubber particles. Filled and open symbols represent data for PVC–NBR 16 and PVC–NBR 26 blends, respectively.

2.7. Examinations of deformation mechanisms

The fractured surfaces of PVC–NBR 18 and PVC–NBR 26 blends generated during Izod impact tests were coated with gold and observed on a Hitachi S-530 SEM.

The internal damaged zone of a tough PVC–NBR 18 blend was examined on a Hitachi S-530 SEM and a Hitachi H-800 transmission electron microscope (TEM). The internal damaged zone of a tough PVC–NBR 26 blend was observed on a Hitachi S-560 SEM. Microtoming was performed under cryogenic conditions (ca −100°C) using a microtome equipped with a glass knife to give superthin sections. The superthin sections were stained with osmium tetroxide (OsO_4) vapor so that the NBR phase appears to be dark in TEM pictures.

2.8. Measurements of volume strain

The relative volume strain ($\Delta V/V$) is calculated from

$$\Delta V/V = \frac{\rho_b - \rho_w}{\rho_w} \quad (1)$$

where ρ_b is the density of the blend outside the deformed zone, ρ_w the density of the same blend within the deformed zone. These density values were measured by using a gradient column filled with NaBr aqueous solution.

3. Results and discussion

3.1. Morphology

Three types of morphologies in PVC–rubber blends: the morphology of well-dispersed rubber particles, the pseudo-network morphology and the continuous rubber network morphology, are effective in the toughening of PVC but with different toughening efficiencies [14,18–21,32,33]. The variety of morphologies that can be achieved is due to the particulate nature of PVC. The present work focuses on blends with the morphology of well-dispersed rubber particles. This morphology has been achieved by adding a plasticizer and blending at a high temperature (160°C). The morphology of PVC–NBR 18 blends has already been shown in our previous papers [14,20,21]. Fig. 1 shows the SEM micrograph of a PVC–NBR 26 blend. Like the PVC–NBR 18 blends, it has the morphology of well-dispersed rubber particles. All PVC–NBR blends studied in this work have the same dispersion state, the morphology of well-dispersed NBR rubber particles.

The particle sizes of all PVC–NBR 26 blends fit the log–normal distribution. The values of particle size distribution parameter σ for PVC–NBR 26 blends lie between 1.5 and 1.7, and are close to those for PVC–NBR 18 blends. Fig. 2 shows the variation of rubber particle size d (at the probability of 50% in a log–normal plot) with rubber volume fraction ϕ for PVC–NBR 18 (open symbols) and PVC-NBR 26 (filled symbols) blends. For a given ϕ, the d values for PVC–NBR

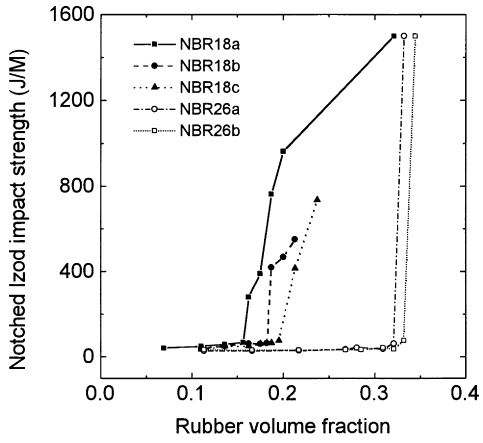

Fig. 3. Notched Izod impact strength versus rubber volume fraction for PVC–NBR blends with the morphology of well-dispersed rubber particles. Filled and open symbols represent data for PVC–NBR 16 and PVC–NBR 26 blends, respectively.

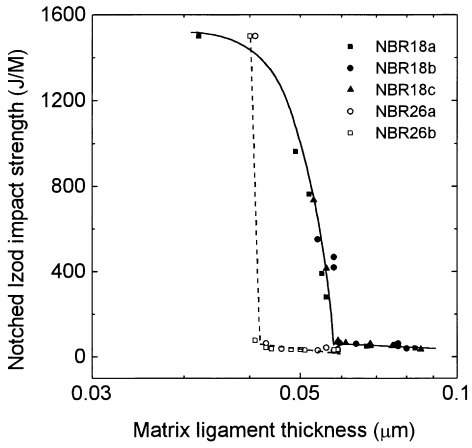

Fig. 4. Notched Izod impact strength versus matrix ligament thickness for PVC–NBR blends with the morphology of well-dispersed rubber particles. Filled and open symbols represent data for PVC–NBR 18 and PVC–NBR 26 blends, respectively.

26 blends are smaller than those for PVC–NBR 18 blends. It has been established that d decreases with increasing interfacial adhesion when other influential factors are identical [56,57]. Since all the blends have been prepared under the same processing conditions, the smaller d values for PVC–NBR 26 blends can be attributed to the stronger interfacial adhesion between PVC and NBR phases when the NBR rubber has a higher AN content. It is also seen that d increases with increasing ϕ. Wu et al. [56,57] have established models to correlate polymer particle size with other parameters for polymer blends. Moreover, Serpe and coworkers [57] have shown that the rubber particle size is a function of rubber content. The variation of rubber particle size with rubber volume fraction in this work basically supports the model proposed by Serpe and coworkers [57]. Fig. 2 also shows that it is easier to change the rubber particle size in PVC–NBR 18 blends by milling NBR.

3.2. Brittle–ductile transition master curves

The notched Izod impact strength as a function of ϕ for PVC–NBR 18 and PVC–NBR 26 blends is depicted in Fig. 3. Brittle–ductile transitions occur for all the blends. For PVC–NBR 18 blends, the critical rubber volume fractions ϕ_c at which the transition occurs increases with increasing milling time, i.e. ϕ_c increases with increasing d (compare Fig. 3 with Fig. 2). The brittle–ductile transition for PVC–NBR 26 blends is sharper, and takes place at much higher ϕ_c than PVC–NBR 18 blends. Since milling has little effect on the d values of PVC–NBR 26 blends, PVC–NBR 26a and PVC–NBR 26b have essentially the same ϕ_c value.

The above data on PVC–NBR blends and the results for other blends [1–30] clearly show that the toughness depends on d, σ and ϕ. The effects of these morphological parameters can be combined as the effect of a single parameter, the matrix ligament thickness T, which is given by [53–55]

$$T(d,\sigma,\phi) = d\left[\xi\left(\frac{\pi}{6\phi}\right)^{1/3}\exp(1.5\ln^2\sigma) - \exp(0.5\ln^2\sigma)\right] \quad (2)$$

where ξ is taken as one in the present work. It has been pointed out that the d value at a probability of 50% in a log–normal plot rather than the number- or weight-average d should be used for calculating T in Eq. (2).

Fig. 4 shows the notched Izod impact strength as a function of T. It is clear that all the data points for each blend (e.g. PVC–NBR 18) fall on a master curve. The critical ligament thicknesses T_c for brittle–ductile transition are $T_{c1} = 0.059$ μm and $T_{c1} = 0.041$ μm or PVC–NBR 18 and PVC–NBR 26 blends, respectively. Between $T = 0.041$ and 0.059 μm PVC–NBR 26 blends are still in the brittle state and thus have impact strengths much lower than those of PVC–NBR 18 blends. We have demonstrated that a small T_c is unfavorable for toughening [11]. Consequently, an increase of AN level from 18 to 26 wt% is disadvantageous for the toughening of PVC. Why the interfacial adhesion between PVC and NBR has such an effect on the impact strength of the blends must be found out according to the deformation mechanisms of the blends as discussed in the next part of this work.

3.3. Deformation behavior

3.3.1. Izod impact fractured surfaces

Discontinuous bands, indicative of brittle fracture, are usually observed on impact fractured surface of a rigid PVC sample. However, they disappear gradually with the addition of rubber. Fibrils are easily observed on the fractured surface of tough PVC–NBR 18 blends. We have shown that the array of fibrils is influenced by the spatial distribution of rubber particles [20]. For a supertough blend with the morphology of well-dispersed particles,

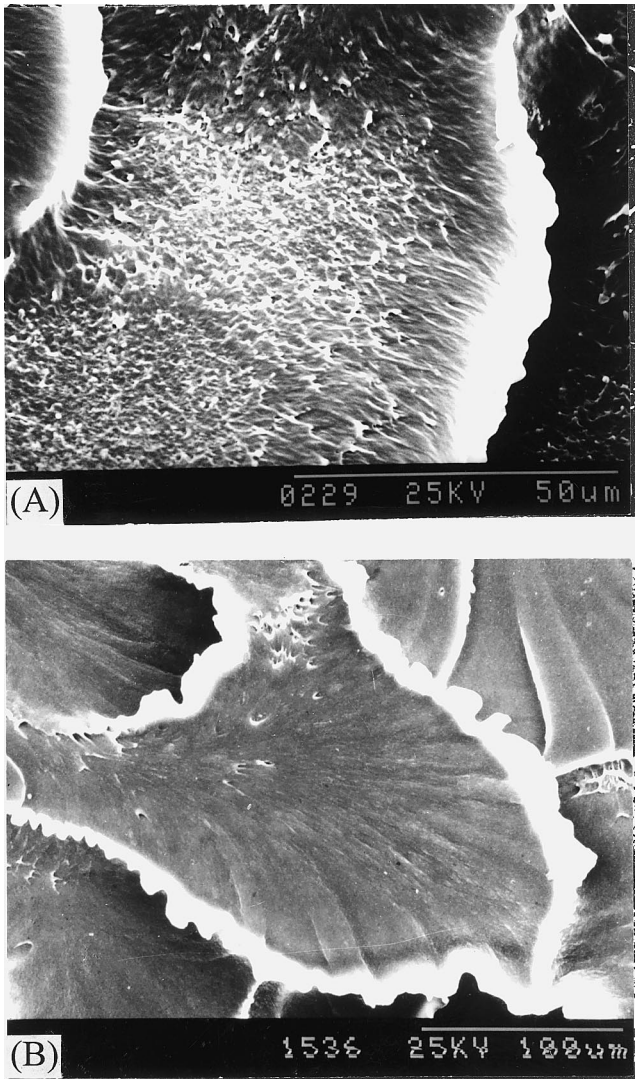

Fig. 5. SEM micrographs of the Izod impact fractured surfaces. (A) Tough PVC–NBR 18 blend with $d = 0.105$ μm, $T = 0.058$ μm and notched Izod impact strength = 418 J m^{-1}. (B) PVC–NBR 26 blend with $d = 0.1$ μm, $T = 0.040$ μm and notched Izod impact strength ≈ 1500 J m^{-1}.

fibrils are uniformly distributed on the fractured surface. For a supertough blend with the pseudo-network morphology, fibrils are seen between PVC primary particles.

Fig. 5 shows the fractured surfaces of two supertough PVC–NBR blends with different interfacial adhesion strength, which were formed during Izod impact tests at room temperature. Large number of fibrils and voids are uniformly distributed on the Izod impact fractured surface of the supertough PVC–NBR 18 blend (Fig. 5A). This figure also suggests that crazing on the fractured surface of the supertough PVC–NBR 18 blend takes place during crack propagation. However, very few fibrils and voids are seen on the Izod impact fractured surface of the supertough PVC–NBR 26 blend (Fig. 5B). No craze is formed on the fractured surface of the supertough PVC–NBR26 blend during crack propagation. Therefore, different interfacial adhesion between PVC and NBR leads to quite different

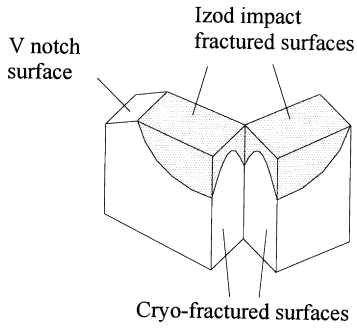

Fig. 6. Schematic illustration of the preparation of samples used for examination of deformation mechanisms in PVC–NBR blends by using SEM and TEM, respectively. The dotted areas represent the deformation region.

fractured surfaces even though the two blends have the same morphology of well-dispersed rubber particles.

3.3.2. Microvoiding mechanism

Stress whitening was observed in all deformed tough PVC–NBR18 blends but not in all deformed tough PVC–NBR 26 blends. It arises from the formation of voids within the deformed zone. The volume strain $\Delta V/V$ for the PVC–NBR 18 blend with $T = 0.054$ μm and notched Izod impact strength of 550 J m^{-1} is 0.025, indicating that there are voids in this sample. But the $\Delta V/V$ value for the PVC–NBR 26 blend with $T = 0.040$ μm and notched Izod impact strength of 1500 J m^{-1} is zero, indicating that there is no void in this sample. Likewise, Havriliak and coworkers [58] reported that there is no internal cavitation of MBS particles nor debonding at the PVC–MBS interface in tough PVC–MBS blends until after the particles have been deformed by the fracture process.

The preparation and observation locations of samples used for examinations of deformation mechanisms are illustrated in Fig. 6. The dotted areas denote the stress-whitened region in the supertough PVC–NBR 18 blends. However, the supertough PVC–NBR 26 blends did not show any stress whitening. Therefore, the dotted areas only denote the deformation region. A sharp notch of about 0.5 mm in depth was made on the sample by using a razor blade after an Izod impact test. The sample having the sharp notch was cooled in liquid nitrogen, and then quickly fractured. The cryo-fractured surface was coated with gold for SEM observations.

Fig. 7 shows the SEM observations on the cryo-fractured surface of the PVC–NBR 18c blend with $d = 0.105$ μm, $T = 0.058$ μm and notched Izod impact strength of 418 J m^{-1}. A–D are located along the symmetrical axis of the cryo-fractured surface, with locations C and D in the deformation region. E–G are near the surface of the compression-molded sample, with locations E and F in the deformation region.

Fig. 7A was taken at location A, which is far away from the stress-whitened region. Some holes (appearing as black

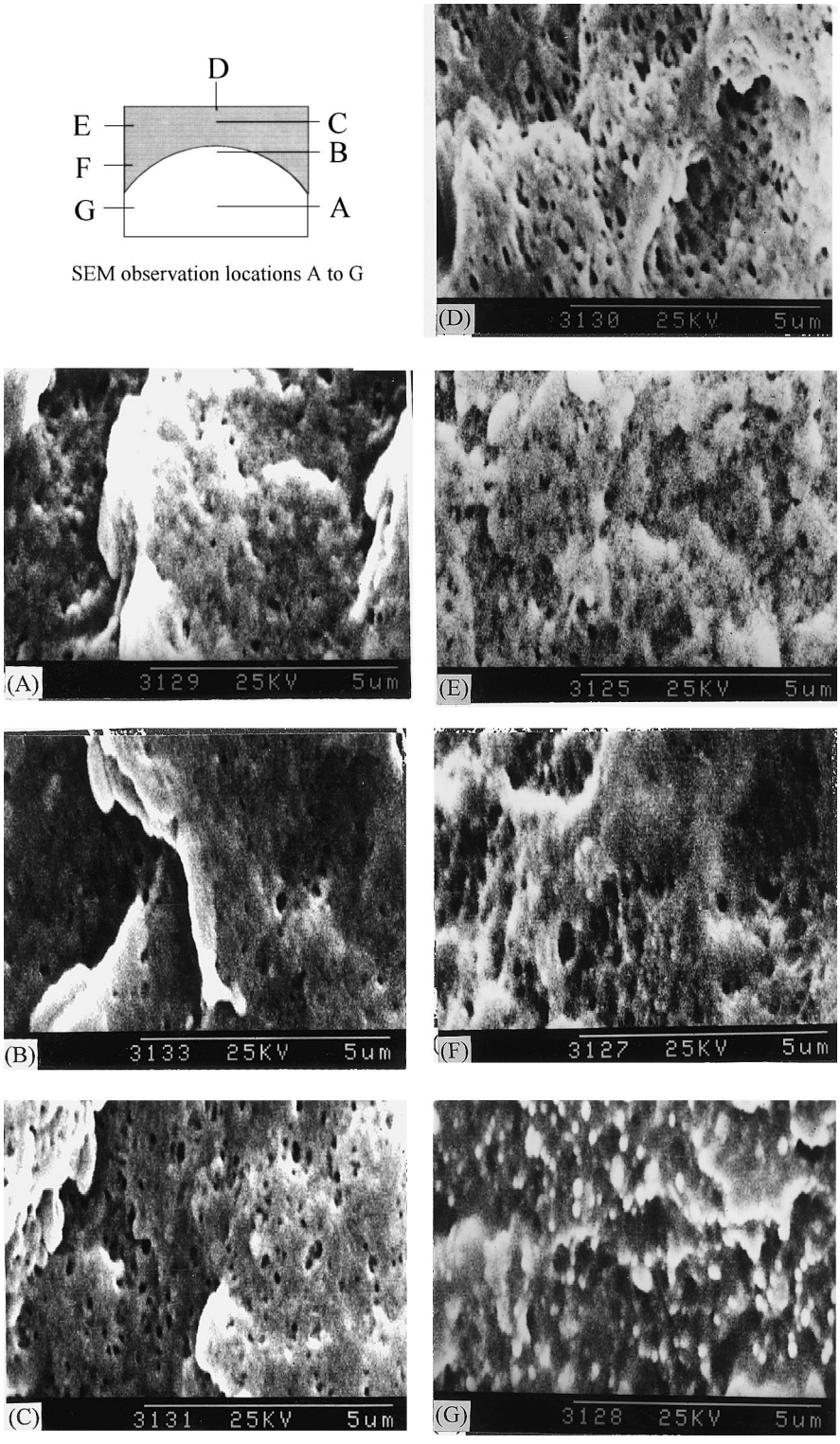

Fig. 7. SEM micrographs of the cryo-fractured surface of a tough PVC–NBR 18 blend with $d = 0.105$ μm, $T = 0.058$ μm and notched Izod impact strength = 418 J m^{-1}. The location of the observed surface is illustrated in Fig. 6.

dots) are seen, indicating that NBR 18 particles were detached from the surface during the cryo-fracture process. Location B is close to but outside the stress-whitened zone. Some dark dots and white dots are seen (Fig. 7B), which are similar to those observed in Fig. 7A. Locations C and D are in the stress-whitened zone and are about 100 and 50 μm away from the Izod impact fractured surface, respectively. A great number of holes are seen in Fig. 7C and D. These

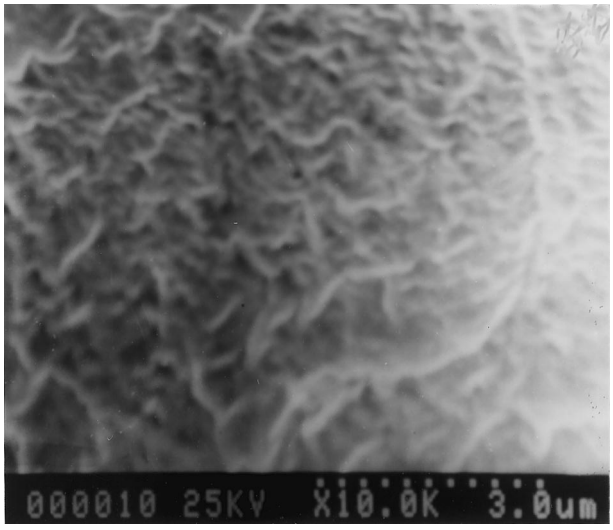

Fig. 8. SEM micrograph of the cryo-fractured surface of a tough PVC–NBR26 blend with $d = 0.1$ μm, $T = 0.040$ μm and notched Izod impact strength ≈ 1500 J m^{-1}. The location of the observed surface is illustrated in Fig. 6.

holes arise not only from the detachment of NBR 18 particles but also from debonding at the PVC–NBR 18 interface (revealed by TEM observations). Locations E and F (40 μm and 1 mm away from the Izod impact fractured surface, respectively) are in the deformation region. Holes and NBR 18 particles are found (see Fig. 7E and F). Interestingly, a large number of NBR 18 particles but a small number of holes are seen in the undeformed region near the surface made by compression molding (Fig. 7G). Therefore, the NBR 18 particles are not well bonded to the PVC matrix.

Fig. 8 shows the SEM observation on the cryo-fractured surface of the PVC–NBR 26a blend with $d = 0.094$ μm, $T = 0.040$ μm and notched Izod impact strength of 1500 J m^{-1}. This picture was taken in the deformation zone of the sample. No hole can be found on the cryo-fractured surface of the sample, implying that the NBR 26 particles are well bonded to the PVC matrix and are not easily detached during the cryo-fracture process.

The results shown in Figs. 7 and 8 suggest that the interfacial adhesion at the PVC–NBR18 interface is moderate and that at the PVC–NBR 26 interface is strong. This conclusion is consistent with that reached from the variation of the rubber particle size with the AN content in NBR. Fig. 8 also suggests that the main toughening mechanism for PVC–NBR 26 blends is matrix shear yielding.

TEM measurements were performed on the PVC–NBR 18 blends to find out the microvoiding mechanism in the blends. The surface of the superthin section used for TEM observations is parallel to the cryo-fractured surface (see Fig. 6). Fig. 9 shows the TEM micrographs of the PVC–NBR 18c blend for which the SEM micrographs have been shown in Fig. 7. Fig. 9A was taken at location A (in the undeformed region). Rubber particles appear to be dark owing to staining with OsO_4. There is no void in this region, suggesting that the voids observed in the following pictures do not result from the microtoming processes. Many voids together with highly elongated rubber particles are seen in Fig. 9B taken at location B close to the Izod impact

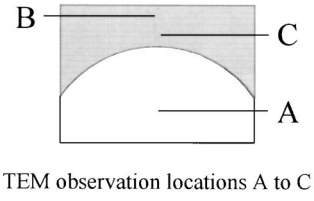

TEM observation locations A to C

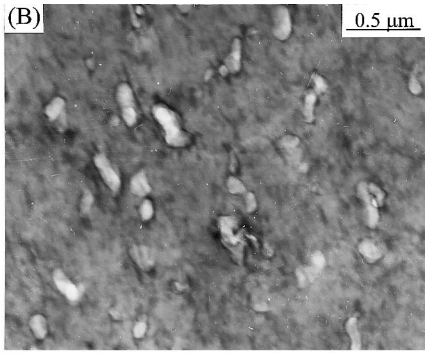

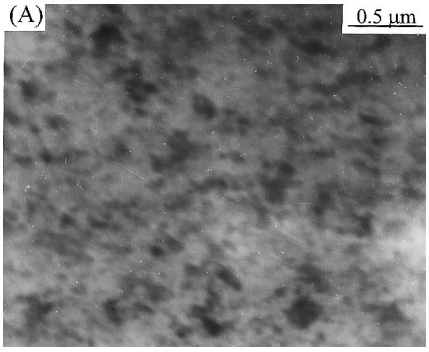

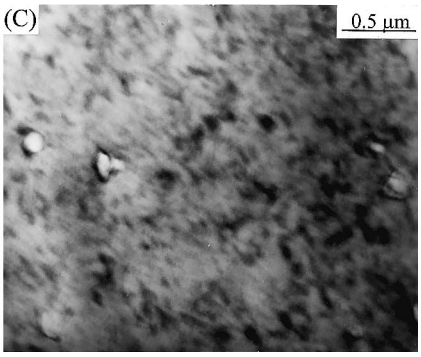

Fig. 9. TEM micrographs of a tough PVC–NBR 18 blend with $d = 0.105$ μm, $T = 0.058$ μm and notched Izod impact strength of 418 J m^{-1}.

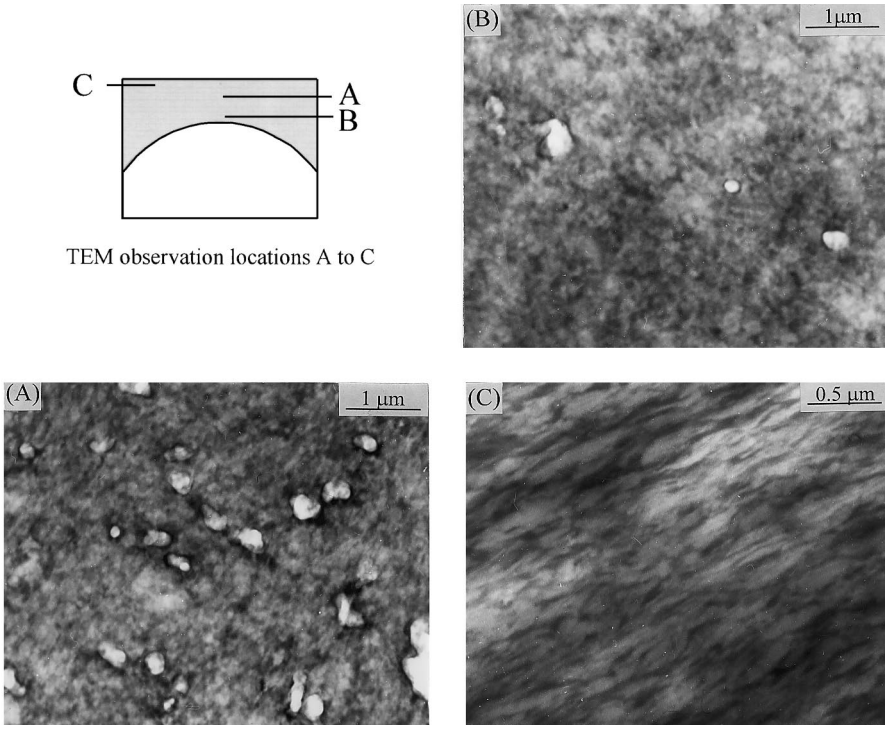

Fig. 10. TEM micrographs of a supertough PVC–NBR 18a blend with $d = 0.12$ μm, $\phi = 0.321$, $T = 0.032$ μm and notched Izod impact strength ≈ 1500 J m^{-1}.

fractured surface. This picture is quite different from those reported in literature where a rubber shell encapsulates a void. In our case, no void is fully encapsulated by the rubber phase, and debonding at the PVC–NBR 18 interface is clearly seen. Fig. 9C, taken at location C, also clearly shows the mechanism of debonding at the PVC–NBR 18 interface.

TEM observations (Fig. 10) was also made on the PVC–NBR 18a blend with $d = 0.12$ μm, $\phi = 0.321$, $T = 0.032$ μm and notched Izod impact strength ≈ 1500 J m^{-1}. Fig. 10A was taken at location A (near the center of the deformation region). The voids in this blend look like those in the blend shown in Fig. 9B. A smaller number of voids are seen in Fig. 10B taken at location B (in the deformation region but far from the Izod impact fractured surface). The voids in this blend should also arise from debonding at the PVC–NBR 18 interface. It was noticed that there was a small area on the Izod impact fractured surface of the blend where stress whitening disappeared. It is hard to see any void in Fig. 10C taken at location C (in the deformation region). With small rubber particle size, it is generally difficult for internal cavitation of rubber particles to take place. Therefore, the stress whitening observed in all tough PVC–NBR 18 blends is attributable to debonding at the PVC–NBR 18 interface.

In general, crazing and shear yielding in the polymer matrix are the two major energy absorption mechanisms in polymer blends containing dispersed particles [59,60]. For the tough PVC–NBR 18 blends studied in this work, the deformation region just beneath the impact fractured surface is large and it absorbs the major amount of impact energy. Since crazes have not been seen in the deformation region, the main energy absorption mechanism in the tough PVC–NBR 18 blends is matrix shear yielding.

Too small rubber particle size was found to lower the toughening efficiency in PVC-rubber [29–34,51,52] and other plastic–rubber [35,36,49,50] blends. Dompas and coworkers [29,51,52] suggested that the minimum rubber particle size for internal cavitation of MBS particles in PVC–MBS blends is about 0.15 μm. However, Takaki and coworkers [30] reported that in PVC–MBS blends MBS particles of 0.084 μm are able to cavitate internally. For PVC–NBR blends, we have not observed any internal cavitation of rubber particles in the investigated particle size range of 0.04–0.12 μm, so the minimum rubber particle size for the occurrence of internal cavitation must be greater than 0.12 μm.

In the present work, a PVC–NBR 18a blend with $d = 0.073$ μm, $\phi = 0.162$ and $T = 0.056$ μm has an impact strength of 280 J m^{-1}, which is much higher than that (30 J m^{-1}) of pure PVC. Moreover, Mathur and Vanderheiden [61,62] reported that PVC containing $CaCO_3$ particles of diameter $d = 0.07$ μm is supertough. Therefore, the minimum particle size of NBR or $CaCO_3$ for achieving toughening effect must be smaller than 0.073 μm.

It has been proposed that debonding at the interface between the rubber phase and the matrix is equally

effective in toughening as the internal cavitation of the rubber phase [28,63–65]. This is because debonding also relieves the triaxial tension ahead a crack, thereby promoting shear yielding of the matrix. This mechanism is responsible for the high toughening efficiency of PVC–$CaCO_3$ [61,62] and HDPE–$CaCO_3$ [8,16] composites. All NBR rubbers used in this work have the same glass transition temperature (50 ± 1°C) and their mechanical properties at room temperatures should be roughly the same and thus would not affect toughening. Therefore, the observed difference between the two master curves in the range of $0.041\ \mu m \leq T \leq 0.059\ \mu m$ (see Fig. 4) stems from the change in the interfacial adhesion between PVC and NBR.

4. Conclusions

As the AN content in NBR increases from 18 to 26 wt%, the interfacial adhesion between PVC and NBR increases, and the size of rubber particles decreases. The present study shows that the effects of morphological parameters and interfacial adhesion on the impact toughness of PVC–NBR blends are interrelated. The effect of morphology for a uniform dispersion of rubber particles can be expressed in terms of a single parameter, the matrix ligament thickness T. The effect of interfacial adhesion can be separated by plotting the impact strength against T. PVC–NBR 18 (with medium interfacial adhesion) undergoes a brittle–ductile transition at $T_c = 0.059\ \mu m$ while PVC–NBR 26 (with stronger interfacial adhesion) has a similar transition at $T_c = 0.041\ \mu m$. Hence, an adverse direct effect of strengthening interfacial adhesion is the lowering of impact strength in the range $0.041\ \mu m \leq T \leq 0.059\ \mu m$.

SEM studies of the cryo-fractured surfaces inside the deformed zones of tough PVC–NBR blends also reveal that NBR 18 and NBR 26 rubbers have medium and strong interfacial adhesion with PVC, respectively. TEM observations show that debonding at the PVC–NBR 18 interface is the predominant deformation mechanism. However, as revealed by density and SEM measurements no cavitational event takes place in PVC–NBR 26 blends.

The interfacial adhesion between PVC and NBR has a direct influence on the deformation behavior of PVC–NBR blends. The main energy absorption mechanism for both PVC–NBR 18 and 26 blends is matrix shear yielding. The debonding at the PVC–NBR 18 interface promotes the shear yielding of the PVC matrix. However, the absence of cavitation in PVC–NBR 26 blends delays the occurrence of extensive matrix yielding.

Acknowledgements

Dr Zhehui Liu wishes to acknowledge the support of the Hong Kong Polytechnic University Postdoctoral Fellowship Scheme. We wish to thank the NSFC (China) and the Hong Kong Research Grant Council for financial supports.

References

[1] Wu S. Polymer 1985;26:1855.
[2] Wu S. J Appl Polym Sci 1988;35:549.
[3] Wu S. Polym Engng Sci 1990;30:753.
[4] Wu S. Polym Int 1992;29:229.
[5] Flexman EA. Mod Plast 1985;62:72.
[6] Jancar J, DiAnselmo A, DiBenedetto AT. Polym Commun 1991; 32:367.
[7] Wu XZ, Zhu XG, Qi ZN. In: Proceedings of the Eighth International Conference on Deformation, Yield and Fracture of Polymers, London, 1991, p. 78/1.
[8] Fu Q, Wang GH, Shen JS. J Appl Polym Sci 1993;49:673.
[9] Starke JU, Michler GH, Grellmann W, Seidler S, Gahleitner M, Feibig J, Nezbedova E. Polymer 1998;39:75.
[10] Kim GM, Michler GH, Gahleitner M, Fiebig J. J Appl Polym Sci 1996;60:1391.
[11] Liu ZH, Zhang XD, Zhu XG, Qi ZN, Wang FS. Polymer 1998; 39:1863.
[12] Jiang W, Liu CH, Wang ZG, An LJ, Liang HJ, Jiang BZ, Wang XH, Zhang HX. Polymer 1998;39:3285.
[13] Jiang W, Liang HJ, Jiang BZ. Polymer 1998;39:4473.
[14] Liu ZH, Zhang XD, Zhu XG, Qi ZN, Wang FS, Li RKY, Choy CL. Polymer 1998;39:5019.
[15] Bartczak Z, Argon AS, Cohen RE, Weinberg M. Polymer 1999; 40:2331.
[16] Bartczak Z, Argon AS, Cohen RE, Weinberg M. Polymer 1999; 40:2347.
[17] Borggreve RJM, Gaymans RJ, Schuijer J, Ingen Housz JF. Polymer 1987;28:1489.
[18] Breuer H, Haaf F, Stabenow J. J Macromol Sci Phys 1977;B14:387.
[19] Haaf F, Breuer H, Stabenow J. Angew Makromol Chem 1977;58/ 59:95.
[20] Liu ZH, Zhang XD, Zhu XG, Qi ZN, Wang FS, Li RKY, Choy CL. Polymer 1998;39:5027.
[21] Liu ZH, Zhang XD, Zhu XG, Qi ZN, Wang FS, Li RKY, Choy CL. Polymer 1998;39:5035.
[22] Michler GH, Starke JU. In: Riew CK, Kinloch AJ, editors. Toughened plastics II: New approaches in science and engineering, Advances in chemistry series, 252. Washington, DC: American Chemical Society, 1996. p. 251.
[23] Liu NC, Baker WE. Polym Engng Sci 1992;32:1695.
[24] Cho K, Yang J, Park CE. Polymer 1997;38:5161.
[25] Borggreve RJM, Gaymans RJ. Polymer 1989;30:63.
[26] Gaymans RJ, Dijkstra K, ten Dam MH. In: Riew CK, Kinloch AJ, editors. Toughened plastics II: Novel approaches in science and engineering, Advances in chemistry series, 252. Washington, DC: American Chemical Society, 1996. p. 303.
[27] Lovell RA, Sherratt MM, Yong RJ. In: Riew CK, Kinloch AJ, editors. Toughened plastics II: Novel approaches in science and engineering, Advances in chemistry series, 252. Washington, DC: American Chemical Society, 1996. p. 211.
[28] Dompas D, Groeninckx G, Isogawa M, Hasegawa T, Kadokura M. Polymer 1995;36:437.
[29] Dompas D, Groeninckx G, Isogawa M, Hasegawa T, Kadokura M. Polymer 1994;35:4760.
[30] Takaki A, Yasui H, Narisawa I. Polym Engng Sci 1997;37:105.
[31] Dunkelberger DL, Dougherty EP. J Vinyl Tech 1990;12:212.
[32] Matsuo M, Nozaki C, Jyo Y. Polym Engng Sci 1969;9:197.
[33] Matsuo M. Japan Plats, 1968; July 6.
[34] Morton M, Cizmecioglu M, Lhila R. Adv Chem Ser 1984;206:221.
[35] Oostenbrink AJ, Molenaar LJ, Gaymans RJ. Polyamide–rubber

blends: influence of very small rubber particle size on impact strength. Poster given at the Sixth Annual Meeting of the Polymer Processing Society, Nice, France, 18–20 April 1990.
[36] Oshinski AJ, Keskkula H, Paul DR. Polymer 1992;33:268.
[37] Keskkula H, Kim H, Paul DR. Polym Engng Sci 1990;30:1373.
[38] Kim H, Keskkula H, Paul DR. Polymer 1990;31:869.
[39] Majumdar B, Keskkula H, Paul DR. Polymer 1994;35:3164.
[40] Majumdar B, Keskkula H, Paul DR. Polymer 1994;35:5453.
[41] Majumdar B, Keskkula H, Paul DR. Polymer 1994;35:5468.
[42] Brady AJ, Keskkula H, Paul DR. Polymer 1994;35:3665.
[43] Kayano Y, Keskkula H, Paul DR. Polymer 1996;37:4505.
[44] Angola JC, Fujita Y, Sakai T, Inoue T. J Polym Sci Polym Phys Ed 1988;26:807.
[45] Hobbs SY, Bopp RC, Watkins VH. Polym Engng Sci 1983;23:380.
[46] Liu NC, Baker WE. Polymer 1994;35:988.
[47] Kayano Y, Keskkula H, Paul DR. Polymer 1997;38:1885.
[48] Kayano Y, Keskkula H, Paul DR. Polymer 1998;39:2835.
[49] Lazzeri A, Bucknall CB. J Mater Sci 1993;28:6799.
[50] Lazzeri A, Bucknall CB. J Mater Sci 1994;29:3377.
[51] Dompas D, Groeninckx G. Polymer 1994;35:4743.
[52] Dompas D, Groeninckx G, Isogawa M, Hasegawa T, Kadokura M. Polymer 1994;35:4750.
[53] Liu ZH, Zhang XD, Zhu XG, Li Q, Qi ZN, Wang FS. Polymer 1997;38:5267.
[54] Liu ZH, Li RKY, Tjong SC, Qi ZN, Wang FS, Choy CL. Polymer 1998;39:4433.
[55] Liu ZH, Li RKY, Tjong SC, Choy CL, Zhu XG, Qi ZN, Wang FS. Polymer 1999;40:2903.
[56] Wu S. Polym Engng Sci 1987;27:335.
[57] Serpe G, Jarrin J, Dawans F. Polym Engng Sci 1990;30:553.
[58] Havriliak Jr S, Cruz CA, Slavin SE. Polym Engng Sci 1996;36:2327.
[59] Bucknall CB. Toughened plastics. London: Applied Science, 1977.
[60] Kinloch AJ, Young RJ. Fracture behavior of polymers. London: Applied Science, 1983.
[61] Mathur KK, Vanderheiden DB. In: Kresta JE, editor. Polymer science and technology, Polymer additives. New York: Plenum Press, 1984. p. 371.
[62] Mathur KK, Driscoll SB. J Vinyl Tech 1982;4:81.
[63] Sue HJ, Huang J, Yee AF. Polymer 1992;33:4868.
[64] Huang Y, Kinloch AJ, Bertsch RJ, Siebert AR. In: Riew CK, Kinloch AJ, editors. Toughened plastics I: Science and engineering, Advances in chemistry series, 233. Washington, DC: American Chemical Society, 1993. p. 189.
[65] Kim GM, Michler GH. Polymer 1998;39:5689.